Article

Chemotherapeutics Combined with Luminal Irritants: Effects on Small-Intestinal Mannitol Permeability and Villus Length in Rats

Maria-José Cano-Cebrián [1,2,†] **, David Dahlgren** [2,†] **, Fredrik Kullenberg** [2] **, Karsten Peters** [2] **, Tobias Olander** [2] **, Markus Sjöblom** [3] **and Hans Lennernäs** [2,*]

1 Department of Pharmacy, Pharmaceutical Technology and Parasitology, University of Valencia, 46100 Burjasot, Spain; Maria.Jose.Cano@uv.es
2 Department of Pharmaceutical Biosciences, Translational Drug Discovery and Development, Uppsala University, 752 36 Uppsala, Sweden; david.dahlgren@farmbio.uu.se (D.D.); Fredrik.kullenberg@farmbio.uu.se (F.K.); Karsten.peters@farmbio.uu.se (K.P.); olander92@hotmail.com (T.O.)
3 Department of Medical Cell Biology, Division of Physiology, Uppsala University, 751 23 Uppsala, Sweden; markus.sjoblom@neuro.uu.se
* Correspondence: hans.lennernas@farmbio.uu.se
† Shared first authorship.

Abstract: Chemotherapy causes intestinal mucositis, which includes villous atrophy and altered mucosal barrier function. However, there is an uncertainty regarding how the reduced small-intestinal surface area affects the mucosal permeability of the small marker probe mannitol (MW 188), and how the mucosa responds to luminal irritants after chemotherapy. The aims in this study were to determine (i) the relationship between chemotherapy-induced villus atrophy and the intestinal permeability of mannitol and (ii) how the mucosa regulate this permeability in response to luminal ethanol and sodium dodecyl sulfate (SDS). This was investigated by treating rats with a single intraperitoneal dose of doxorubicin, irinotecan, or 5-fluorouracil. After 72 h, jejunum was single-pass perfused and mannitol permeability determined at baseline and after 15 min luminal exposure to 15% ethanol or 5 mg/mL SDS. Tissue samples for morphological analyses were sampled from the perfused segment. All three chemotherapeutics caused a similar 30% reduction in villus length. Mannitol permeability increased with irinotecan (1.3-fold) and 5-fluorouracil (2.5-fold) and was reduced with doxorubicin (0.5-fold), suggesting that it is not epithelial surface area alone that regulates intestinal permeability to mannitol. There was no additional increase in mannitol permeability induced by luminal ethanol or SDS in the chemotherapy-treated rats compared to controls, which may be related to the relatively high basal permeability of mannitol compared to other common low-permeability probes. We therefore suggest that future studies should focus on elucidating the complex interplay between chemotherapy in combination with luminal irritants on the intestinal permeability of other probes.

Keywords: chemotherapy-induced mucositis; intestinal permeability; villus atrophy; cytostatics; toxicity; mannitol

1. Introduction

Cancer is the second-largest cause of global premature death before the age of 70, and there is a significant medical need for effective and safe anticancer therapies that will prolong life [1]. Chemotherapeutics kill fast-growing and dividing cancer cells by unselectively inhibiting DNA replication, mitosis, or other important cell cycle functions. This means that proliferating healthy cells throughout the body are also affected. The intestinal mucosa is especially vulnerable because it is completely renewed about once per week by the rapidly dividing stem cells in the crypts of the epithelium [2]. The consequence is off-target gut toxicity, or chemotherapy-induced mucositis (CIM), which is a common condition in cancer patients dosed with anti-neoplastic drugs [3]. Clinically, it is

primarily associated with crippling diarrhea [4], but anorexia, pain, nausea, and sepsis are also common.

In addition to these clinical manifestations, hallmarks of the condition are an impaired absorptive capacity, small intestinal villous atrophy (i.e., a reduction in total epithelial surface area [5]), a lower number of mature enterocytes, and altered intestinal barrier function [6]. In both humans and animal models, the degree of villous atrophy is determined from biopsies. Barrier function, however, is typically measured indirectly by monitoring the plasma exposure and/or renal clearance of non-metabolized paracellular marker probes following oral ingestion [7]. In CIM, the intestinal permeability of the low-molecular-mass probes is assumed to decrease as a result of a reduction in the total intestinal surface area, similar to what is observed with celiac disease [8,9]. However, to our knowledge, no direct measurement has been reported of in vivo intestinal permeability of low-molecular-mass probes following chemotherapy. A direct measurement from the intestines ignores confounding factors in the absorption process, such as gastric emptying, intestinal transit, distribution, and renal elimination. Direct measurements would better clarify the role of different chemotherapeutics in CIM [10] and the complex relationship between mucosal injury and barrier dysfunction in general [11].

Extensive mucosal injury and disease may render the intestinal barrier unrestrictive even to large bacteria [12]. However, under normal conditions, the small intestinal mucosa can handle everyday chemical and mechanical stressors from the luminal side, including high concentrations of bile salts, low pH, and various food components. It can also handle many luminal irritants that are not part of a normal diet, such as ethanol, an organic solvent with central stimulant effects, and sodium dodecyl sulfate (SDS), an anionic surfactant commonly used as a pharmaceutical excipient to optimize drug particle disintegration and dissolution in the GI tract. For instance, small intestinal permeability has been measured in the rat lumen exposed to 15% ethanol w/w [13], or to 5 mg/mL of SDS [14], which corresponds to the upper small intestinal concentrations following oral intake of 80 mL of 40% ethanol [15] or 1 g SDS [16], respectively. The permeability marker ^{51}Cr-EDTA increased noticeably after the luminal exposures but returned to baseline within an hour. This illustrates the remarkable ability of the mucosa to respond to injury and uphold homeostasis even in challenging luminal conditions.

However, a prerequisite for the intestine to rapidly restore a compromised epithelium is a functional restitution process that fills epithelial cellular gaps [17]. An active enteric nervous system is also necessary, as is the normal expression and function of tight junction proteins, which regulate the paracellular transport [18]. Currently, it is not clear what impact chemotherapy has on the normal mucosal injury-response to luminal irritants. A better understanding of these chemotherapeutic effects and the adaptive processes involved in tissue repair is crucial for the development of treatments for CIM, a condition currently lacking effective intervention strategies [19].

The primary objectives of this study were to evaluate the effect of three chemotherapeutics on rat jejunal mucosal histology (villus length and crypt depth), permeability of a low-molecular-mass probe (mannitol), and the relationship between villus length and intestinal permeability. The secondary aim was to evaluate the ability of the jejunum to withstand ethanol- and SDS-induced increases in intestinal permeability following chemotherapy. This was performed by dosing rats with saline or with one of three chemotherapeutics, doxorubicin (DOX), irinotecan (IRI), or 5-fluorouracil (5-FU). After 72 h, when villus atrophy in rodents is reported to be at its greatest [20,21], the jejunum was single-pass perfused with a buffer solution followed by two luminal irritants: ethanol or SDS. During this time, the basal and irritant-induced increase in blood-to-lumen transport of mannitol was monitored. Intestinal samples for histological analysis were sampled adjacent to and inside the perfused segment to evaluate both the effect of chemotherapy alone and in combination with the luminal irritants.

2. Results

2.1. Basal Intestinal Permeability

The mean ($\pm$SEM) baseline $CL_{mannitol}$ over time (the first 0–75 min in each group) for the control ($n = 18$), and DOX, IRI, and 5-FU groups ($n = 12$ each) are presented in Figure 1a. The mean ($\pm$SD) $CL_{mannitol}$ for each rat at steady-state (30–75 min) was used to compare the difference in baseline intestinal permeability between the control and the three chemotherapy groups (Figure 1b). The DOX group had a significantly lower jejunal $CL_{mannitol}$ (1.02 ± 0.94 g mL/min/100 g) compared to the control (1.74 ± 1.06 mL/min/100 g). Conversely, the jejunal $CL_{mannitol}$ was significantly ($p < 0.05$) higher for 5-FU (4.26 ± 2.95 mL/min/100 g). The value for IRI, while higher, was not statistically significant (2.17 ± 1.26 mL/min/100 g).
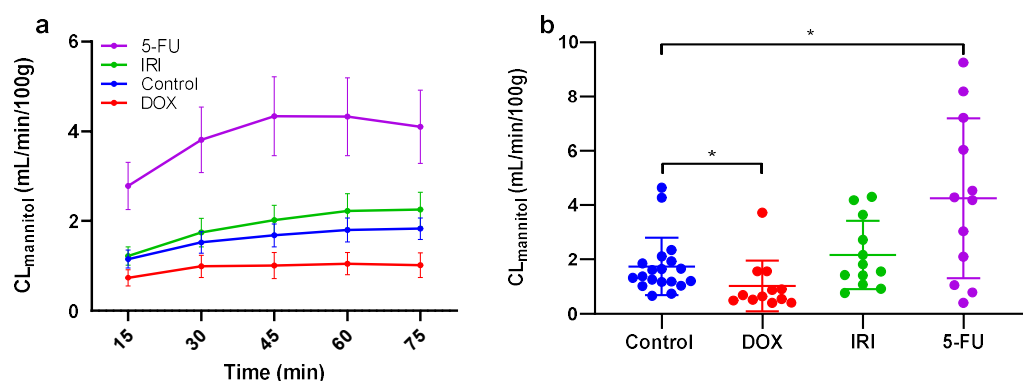

Figure 1. The experiment was performed 72 h after the rats were dosed with saline (control), or with either doxorubicin (DOX), irinotecan (IRI), or 5-fluorouracil (5-FU). (**a**) The mean ($\pm$SEM) blood-to-lumen clearance of mannitol ($CL_{mannitol}$) during single-pass perfusion of the jejunum with a buffer solution during the first 75 min of the perfusion experiment. The average $CL_{mannitol}$ at steady state (between 45 and 75 min) was regarded as representative for each rat. (**b**) The mean ($\pm$SD) and individual $CL_{mannitol}$ values after the different treatments. A * represents a significant difference in $CL_{mannitol}$ between the controls and the chemotherapy-treated rats.

2.2. Villi Length and Crypt Depth

Typical rat jejunal mucosa at control conditions, and at 72 h after chemotherapy, are shown in Figure 2a,b, respectively (only one histological picture following chemotherapy is shown as there were no obvious differences between DOX, IRI, and 5-FU.)
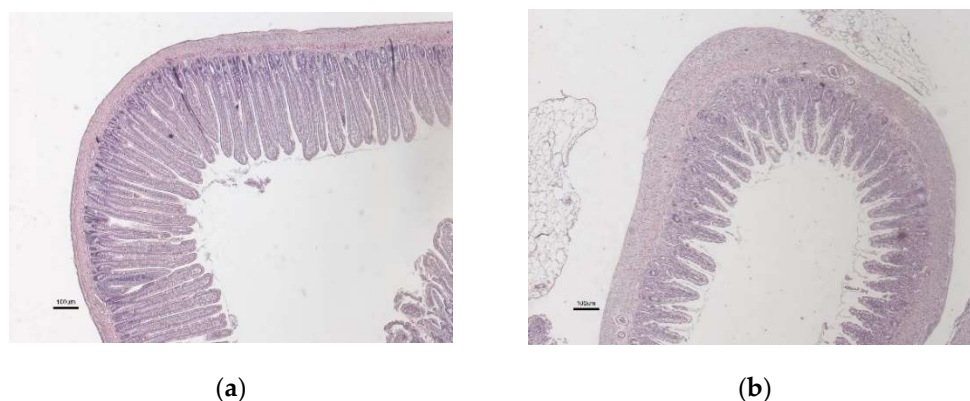

(**a**)   (**b**)

Figure 2. Jejunal mucosa for the (**a**) healthy control rats and (**b**) at 72 h after chemotherapy (there were no obvious differences between DOX, IRI, and 5-FU). Scale bar = 100 µm.

Figure 3a–c shows the mean ($\pm$SD) jejunal villi length, crypt depth, and villi:crypt ratio for the control rats and 72 h after dosing with DOX, IRI, or 5-FU. The villi length decreased significantly ($p < 0.05$) compared to the control (201 ± 24 µM) for all three chemotherapy

groups: DOX (139 ± 27 µM), IRI (144 ± 17 µM), and 5-FU (124 ± 32 µM). For the crypt depth, there were no significant differences for any of the chemotherapies compared to the control group (70 ± 14 µm), but there was a slight increase for DOX (82 ± 15 µm) and IRI (80 ± 17 µm), and a small decrease for 5-FU (63 ± 34 µm). Combining the two morphological measurements (i.e., villi:crypt ratio) gave a significantly ($p < 0.05$) lower ratio compared to the control (3.0 ± 0.6): DOX (1.8 ± 0.3), IRI (1.9 ± 0.6), and 5-FU (2.3 ± 0.7).
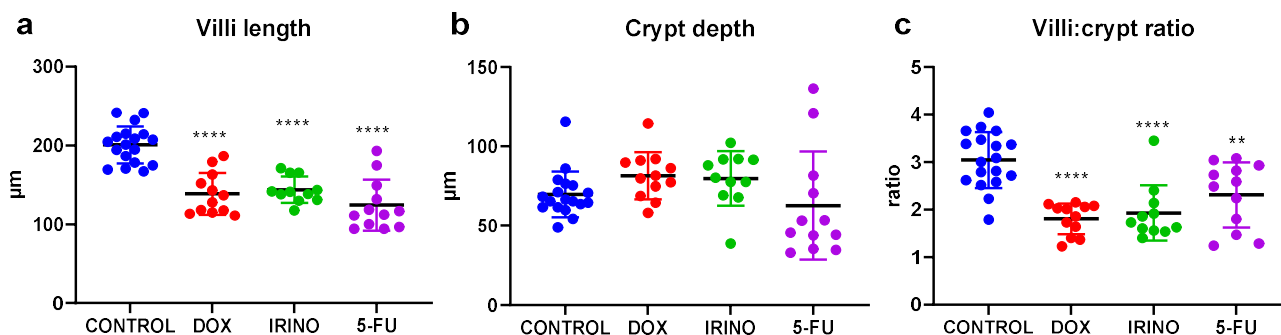

Figure 3. The mean (±SD) and individual (**a**) villus length, (**b**) crypt depth, and (**c**) villi:crypt ratio measured 72 h after the rats were dosed with saline (control), or with either doxorubicin (DOX), irinotecan (IRI), or 5-fluorouracil (5-FU). ** $p < 0.005$ and **** $p < 0.00005$ represent statistically significant differences compared to the control rats.

2.3. Correlation between Basal Intestinal Permeability and Villi Length

Figure 4 shows there was no correlation between villus length (corresponding to surface area) and basal $CL_{mannitol}$ (intestinal permeability) for the combined dataset ($R^2 = 0.1$), or for any of the four individual groups: control ($R^2 = 0.16$), DOX ($R^2 < 0.01$), IRI ($R^2 = 0.16$), or 5-FU ($R^2 = 0.10$).
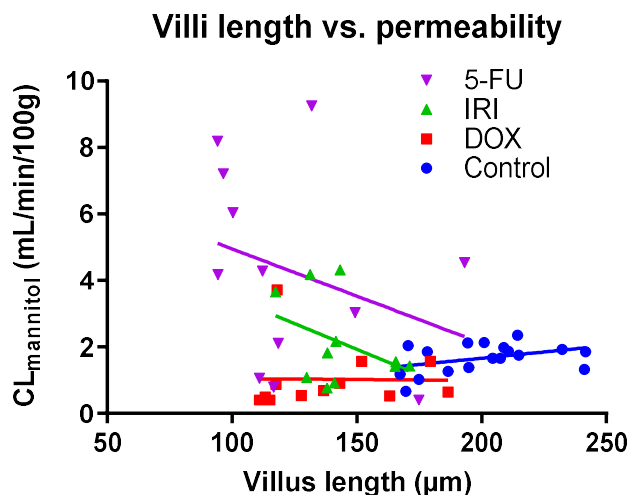

Figure 4. Correlation between villus length and blood-to-lumen clearance of mannitol ($CL_{mannitol}$) in each rat. The determinations were performed 72 h after the rats were dosed with saline (control), or with either doxorubicin (DOX), irinotecan (IRI), or 5-fluorouracil (5-FU).

2.4. Effect of Luminal Irritants on Intestinal Permeability and Histology

The mean (±SEM) $CL_{mannitol}$ values over time (0–150 min) in the control and chemotherapy-treated rats are presented in Figure 5a (ethanol) and Figure 5b (SDS). These irritants were added to the lumen between 75 and 90 min. Ethanol induced a significant ($p < 0.05$), and similar (about twofold), increase in $CL_{mannitol}$ at the end of the 15 min luminal exposure (at 90 min) for all four treatment groups (control, DOX, IRI, and 5-FU)

compared to control rats perfused only with a buffer solution for 150 min. SDS induced no increase in $CL_{mannitol}$ compared to the buffer solution for any of the four treatment groups.
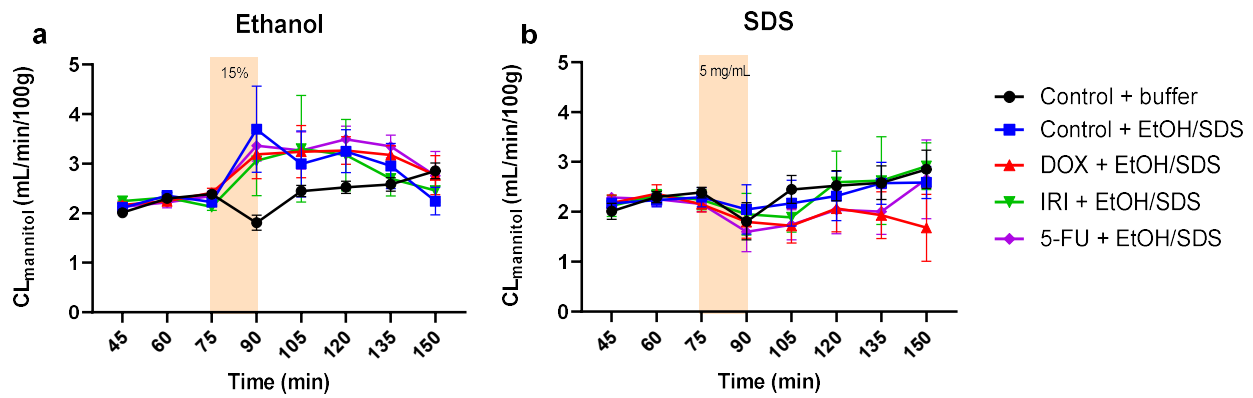

Figure 5. The mean (±SEM) blood-to-lumen clearance of mannitol ($CL_{mannitol}$) during single-pass perfusion of the jejunum with a buffer solution for 75 min, followed by a 15 min perfusion with (**a**) 15% ethanol (EtOH) or (**b**) 5 mg/mL sodium dodecyl sulfate (SDS), followed again with a 60 min perfusion with buffer. The ethanol and SDS perfusions were performed on control rats (blue), and on rats 72 h after treatment with doxorubicin (DOX, red), irinotecan (IRI, green), and 5-fluorouracil (5-FU, purple). The control rats were also perfused with only buffer during 150 min in one group (black).

Intestinal segments perfused with buffer, SDS, or ethanol were analyzed for villi length and crypt depth. In control animals, there was no impact on either villus length or crypt depth from perfusing the segment with a buffer compared to the samples taken adjacent to the perfused segment (Figure 6a). Likewise, there were no differences in villus length or crypt depth induced by SDS or ethanol compared to the buffer. For the chemotherapy-treated rats, there was no effect on villus length of perfusing the intestine with either SDS or ethanol, compared to the adjacent intestinal segment in the same animal (Figure 6b). However, both SDS and ethanol significantly ($p < 0.05$) increased the crypt depth in the DOX- and IRI-treated rats, compared to the adjacent intestinal segment in the same animal (Figure 6c).
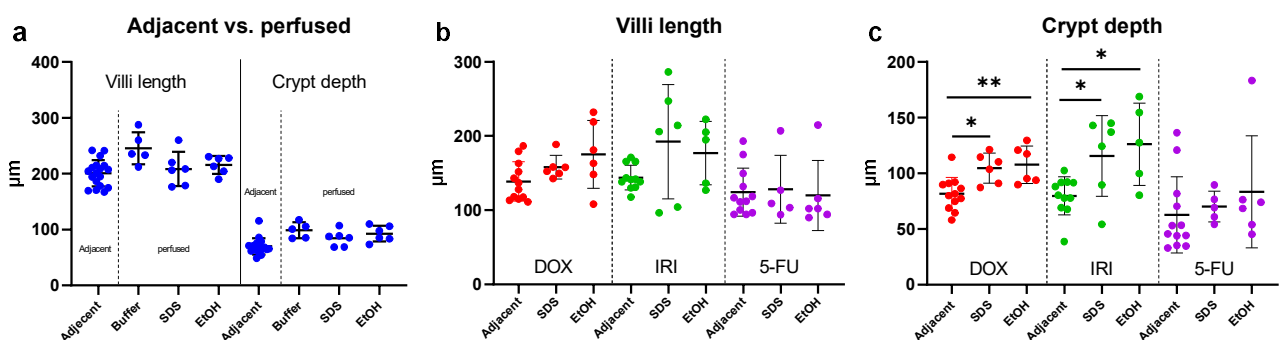
Figure 6. (**a**) Villi length and crypt depth in the non-chemotherapy treated control rats. (**b**) Villi length and (**c**) crypt depth, 72 after treatment with doxorubicin (DOX), irinotecan (IRI) and 5-fluorouracil (5-FU). The adjacent histological segment was sampled outside of the perfused intestinal segment, whereas the other histological segments were sampled 60 min after perfusion with buffer, 15% ethanol (EtOH), or 5 mg/mL sodium dodecyl sulfate (SDS). Data presented as mean (±SD). * $p < 0.05$ and ** $p < 0.005$ represent statistically significant differences between the adjacent and perfused segments.

3. Discussion

This study primarily aimed to elucidate the relationship between chemotherapy-induced villus atrophy and intestinal mucosal mannitol permeability. Secondly, it aimed to

examine the ability of the intestinal mucosa to regulate intestinal mannitol permeability in response to luminal irritants after chemotherapy. This was investigated by treating rats with three different classes of chemotherapeutics: DOX, primarily a topoisomerase II inhibitor; IRI, a topoisomerase I inhibitor; and 5-FU, an antimetabolite. After 72 h, the intestine was single-pass perfused during which the permeability of mannitol was examined before, during, and after luminal exposure to ethanol or SDS. Jejunal tissues for morphological analysis were sampled from both the inside of, and adjacent to, the perfused segment in each rat.

Anti-neoplastic drug therapy is notorious for its severe side effects, in particular chemotherapy-induced intestinal mucositis (CIM). CIM is characterized by morphological changes, such as villus atrophy, together with clinical symptoms of diarrhea, pain, malnutrition, bacterial translocation, and sepsis. The latter two result from therapy-induced immunosuppression in combination with a compromised mucosal barrier. The epithelial barrier status is typically evaluated by measuring the intestinal permeability, which is defined as the ability of the intestine to resist passive transport of water-soluble probes of different sizes and charges. Experimentally, in vivo permeability is usually determined *indirectly* from radioactive or fluorescent probes in plasma or urine following oral dosing [7]. An ideal probe molecule is inert and passively transported in the paracellular pores between cells, which are regulated by tight-junction proteins. However, following oral dosing, the rate and fraction absorbed of a probe also depends on non-permeability factors, such as the gastric emptying rate and intestinal transit time. Both factors can be extensively affected during CIM due to diarrhea. To compensate for these non-permeability factors, probes with different molecular sizes and charges are often combined. Thus, an increased permeability ratio (i.e., large vs. small probe) reflects a reduced surface area and/or increased paracellular leakage [22]. This is based on the assumption that somewhat larger probes, such as ^{51}Cr-EDTA (340 Da) and lactulose (342 Da), are transported only in the leaky pores in the crypt region. The smaller probes, such as mannitol (182 Da), are assumed to be transported paracellularly in the less leaky pores residing over the whole crypt–villus axis [23].

However, the assumption that the surface area reflects epithelial mass transport of mannitol has not been verified in any *direct* determinations of intestinal permeability in relation to CIM. A preclinical method well suited for this evaluation is the SPIP model [24,25]. It relies on transepithelial solute flux at controlled in vivo conditions, in which the intestinal permeability is maintained by hormonal, neural, and paracrine regulation. As such, the SPIP model is often used to investigate intestinal physiology, solute transport, and mucosal injury [26,27]. As rodents are commonly used for evaluating intestinal toxicity of chemotherapy [28], we believe that the rat SPIP model is ideal for evaluating alterations in intestinal permeability in CIM, with or without the presence of luminal irritants.

Following chemotherapy to rodents, maximum histological injury occurs after about three days [20,21]. In our study, all the chemotherapies (DOX, IRI, and 5-FU) decreased the villus length by ≈30% after 72 h, in good agreement with similar studies [29]. Based on the assumption that the primary determinant of intestinal permeability of mannitol is the epithelial surface area available for transport, we expected to see a reduced permeability for all three drugs. Indeed, this was the case for DOX, for which there was a 41% reduction in basal $CL_{mannitol}$. However, for IRI, there was no statistically significant difference compared to the control animals (25% increase), while for 5-FU, basal $CL_{mannitol}$ increased 150%. Furthermore, we were unable to detect any correlation between villus length and $CL_{mannitol}$ for any of the chemotherapy drugs individually, or for the combined dataset. This contradicts the mannitol permeability vs. surface-area paradigm and suggests that other changes important for the intestinal permeability of mannitol are involved. Probably the epithelial leakiness of mannitol increases, at least for 5-FU and IRI. This may be via alteration of the integrity of the epithelial cell monolayer and/or the paracellular junction proteins, as the latter are known to be regulated by proinflammatory cytokines, such as TNFα and IL-4, in the intestines [30]. Thus, it seems that the permeability effects are related

to the individual cytokine profile generated by the different classes of chemotherapeutic drugs used in this study. For instance, IRI and 5-FU generate a strong increase in the proinflammatory cytokines TNFα and IL-1β [31,32]. In contrast, DOX has no effect on TNFα but increases IL-6 sharply [33]. Following 5-FU dosing in mice, a possible relationship is also seen between an increased intestinal permeability of 99mTc-DTPA (MW: 487 Da) and increased expression of TNFα and IL-6 [34]. In summary, our novel *direct* permeability data have implications for the choice of probe, and interpretation of results. This applies to results for permeability studies in general, and for CIM in particular. A better understanding is needed for how different chemotherapeutics and their associated inflammatory and secretory responses affect the intestinal permeability of different probes. This is especially true if intestinal permeability is used as a surrogate endpoint in evaluating the effect of CIM interventions [35].

Our results show that different chemotherapeutics give rise to similar morphological changes. These, in turn, can have substantially different effects on intestinal functions, including membrane transport. The increase in $CL_{mannitol}$ was greatest for 5-FU followed by IRI. Clinically, these are also the two chemotherapeutics that cause the most severe GI disorders [36], especially in combination with each other, causing severe diarrhea in up to 80% of the patients [4]. If these two CIM parameters—increased $CL_{mannitol}$ and diarrhea—are related to each other, the mucosal barrier could be targeted [37] in the treatment of chemotherapy-induced late-onset diarrhea.

Apart from the dysregulation as a result of chemotherapeutics, chronic intestinal barrier dysregulation is seen in many GI and systemic diseases and disorders, such as celiac and inflammatory bowel disease, obesity and type 1 diabetes, non-alcoholic fatty- and alcoholic-liver disease, and irritable bowel syndrome [38]. A healthy intestine forms a selective barrier that balances optimal protection against harmful luminal microorganisms and proteins/xenobiotics/toxins while allowing efficient nutrient absorption. The intestine has a key ability to rapidly respond to, and heal, any injury from luminal irritants and mechanical stress. These irritants may be endogenous, including bile acids from the pancreas or the high acidic load (pH < 2) from the stomach, or originate from oral intake. Two examples from the latter category are ethanol and SDS. Ethanol is an organic solvent with central stimulant effects, and SDS is an anionic surfactant commonly used as a pharmaceutical excipient to optimize drug particle disintegration and dissolution in the GI tract. Both compounds cause local mucosal injury as well as inducing substantial increases in epithelial permeability at physiologically relevant exposure times [18,39]. In a healthy intestine, these changes are repaired within an hour through a functioning restitution process, in combination with a neural and paracrine response system that maintains mucosal (and systemic) homeostasis [3]. There is, however, uncertainty regarding the capability of a chemotherapy-compromised intestine to deal with, and respond to, luminal irritants that normally cause only transient effects.

In this study, ethanol induced a similar twofold increase in $CL_{mannitol}$ in both the control animals and chemotherapy-treated ones, suggesting that anti-neoplastic drug treatment had no impact under the conditions investigated. However, similar to the conclusions from the basal permeability data in this study, the results may be related to the choice of probe. The epithelial membrane may not have sufficiently restricted mannitol transport, thereby making it impossible to detect any difference between the chemotherapy and control groups. For instance, ^{51}Cr-EDTA and inulin are two larger paracellular probes primarily transported in the crypt regions rather than over the whole villus such as mannitol. Both ^{51}Cr-EDTA and inulin have a 5- to 20-fold lower basal permeability in the rat upper small intestine and may thus respond differently than mannitol [23,40]. Indeed, we saw no SDS-induced increase in mannitol permeability in any of the treatment groups, despite the numerous reports of its positive effect on the intestinal permeability of ^{51}Cr-EDTA [18,41].

Even if no significant differences in $CL_{mannitol}$ were detected between the chemotherapy and control groups, the crypt depth increased slightly in the intestinal segment perfused with ethanol and SDS compared to buffer 72 h after dosing with DOX and IRI. The rapid

onset of this increase in crypt depth (150 min) is probably unrelated to the compensatory crypt hyperplasia that is observed about 3–5 days after high doses of stem-cell apoptotic chemotherapy [42]. A more likely explanation is that the luminal irritants trigger mucosal edema. Why this effect was only observed for DOX- and IRI-treated rats, but not the control and 5-FU ones, remains to be investigated. If this increased sensitivity contributes to the mucosal inflammation in CIM, anti-inflammatory treatment is a possible option for CIM interventions.

In conclusion, this study showed that the epithelial surface area was not the only parameter determining the effect of chemotherapy on the intestinal permeability of mannitol. The increase in permeability with IRI and 5-FU, compared to DOX, may explain the severe and frequent diarrhea seen clinically with the former two drugs. In addition, there was no additional increase in mannitol permeability induced by luminal ethanol and SDS in chemotherapy-treated rats compared to the controls. This may be related to the relatively high basal permeability of mannitol compared to other commonly used permeability probes. We therefore suggest that future studies elucidate the complex interplay between different chemotherapeutics and doses in combination with luminal irritants on the intestinal permeability of different probes. Furthermore, an investigation is required to explain the mechanisms behind the increased crypt depth in DOX and IRI-treated rats after luminal exposure to SDS and ethanol.

4. Materials and Methods

4.1. Chemicals

Atropine, Accustain® formalin solution (10%, neutral buffered), dimethyl sulfoxide, ethanol, Inactin (thiobutabarbital sodium), SDS, and bovine albumin were purchased from Sigma-Aldrich (St. Louis, MO, USA). Sodium phosphate dibasic dihydrate ($Na_2HPO_4 \cdot 2H_2O$), potassium dihydrogen phosphate (KH_2PO_4), sodium hydroxide (NaOH), and sodium chloride (NaCl) were purchased from Merck KGaA (Darmstadt, Germany). 5-Fluorouracil Teva (solution for injection, 50 mg/mL), Irinotecan Actavis (solution for infusion, 20 mg/mL), and Dynastat (parecoxib, powder for solution for injection, 40 mg) were purchased from Apoteket AB (Sweden). Doxorubicin hydrochloride was purchased from Toronto Research Chemicals (Toronto, ON, Canada). ^{3}H-Mannitol was purchased from PerkinElmer Life Sciences (Boston, MA, USA).

4.2. Study Formulations

Three chemotherapeutics were used in this study. 5-FU (solution, 50 mg/mL) and IRI (solution, 20 mg/mL) were obtained in ready-to-use form, whereas a 100 mM stock solution of DOX hydrochloride in dimethyl sulfoxide was prepared and diluted to 5 mg/mL in saline on the day of drug administration (final dimethyl sulfoxide concentration < 5%). Parecoxib (10 mg/mL), inactin (50 mg/mL), and atropine (0.1 mg/mL) were dissolved in saline and used within the recommended stability time. For the single-pass intestinal perfusion (SPIP) experiments, three isotonic (290 mOsm) phosphate buffer (8 mM) perfusate solutions were prepared at pH 6.5. The control solution contained only buffer, and two test buffer solutions contained SDS at 5 mg/mL (17.3 mM) or 15% *w/w* ethanol. With the exception of the ethanol solution, osmolarity was determined (after addition of all perfusate constituents) by freeze-point depression using a micro osmometer (Model 3MO; Advanced Instruments, Needham Heights, MA, USA).

4.3. Animals

This rat study was approved by the local ethics committee for animal research (5.8.18-17754/2019) in Uppsala, Sweden. Rats were male Wistar Han IGS from Charles River Co. (France) weighing 340 ± 100 g. They were delivered to the animal laboratory facility in Uppsala, Sweden at least one week before the experiment. Before and during the experiments, the rats were kept in enriched cages with free access to food and water on a 12:12 h light–dark cycle, 21–22 °C.

4.4. Chemotherapy Dosing and Intestinal Perfusions

At 72 ± 2 h before the SPIP permeability experiments, the rats were divided into four treatment groups (Table 1). The control group ($n = 18$) received an intraperitoneal injection of saline, and the three chemotherapy groups ($n = 12$ in each) received a single intraperitoneal injection of either DOX (10 mg/kg, 0.4–0.7 mL), 5-FU (200 mg/kg, 1–2 mL), or IRI (150 mg/kg, 2–3 mL). Immediately before the dosing with IRI, the rats also received a subcutaneous injection with atropine (0.02 mg/rat) to avoid acute and transient cholinergic side effects of this cytostatic prodrug [43,44].

Table 1. The four experimental groups according to the treatment received. See Figure 7 for details of the perfusion. SPIP—single-pass intestinal perfusion; SDS—sodium dodecyl sulfate.

Intraperitoneal Dosing 72 h before SPIP	SPIP Exposure Period (15 min)
Saline, control ($n = 18$)	Buffer ($n = 6$) SDS 5 mg/mL ($n = 6$) Ethanol 15% *w/w* ($n = 6$)
Doxorubicin 10 mg/kg ($n = 12$) or Irinotecan 150 mg/kg ($n = 12$) or 5-Fluorouracil 200 mg/kg ($n = 12$)	SDS 5 mg/mL ($n = 6$) Ethanol 15% *w/w* ($n = 6$)

The surgical procedure and experimental setup of the rat SPIP experiment has been previously described [45]. In short, the rats were anesthetized on the study day using an intraperitoneal injection of a 5% *w/v* inactin solution (180 mg/kg). The body temperature was maintained at 37.5 ± 0.5 °C. The systemic arterial blood pressure was continuously recorded to validate the condition of the animal. This was performed by connecting an arterial catheter to a transducer operating a PowerLab system (AD Instruments, Hastings, UK). Rats with a mean blood pressure below 70 mmHg were excluded from the study. For the SPIP experiment, the abdomen was opened along the midline and a 10–12 cm jejunal segment was cannulated, covered with polyethylene wrap, and placed outside the abdomen [45].

The perfusion study design is illustrated in Figure 7. After completion of surgery, ^{3}H-mannitol was administered intravenously as a bolus of 0.25 µCi (0.1 mL), followed by continuous intravenous infusion at 0.5 µCi per hour (1 mL/h) for the duration of the SPIP experiment. The first 60 min following surgery was a resting period, during which each intestinal segment was perfused with the control buffer solution. This stabilized cardiovascular, respiratory, and intestinal functions, and the ^{3}H-mannitol levels in the plasma.
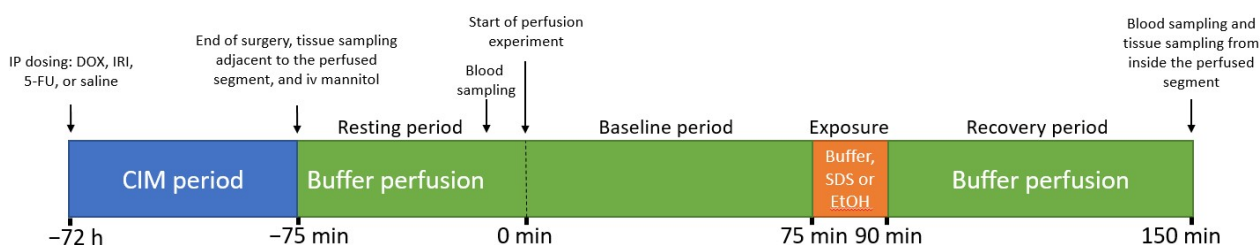

Figure 7. Study design, showing the 72 h chemotherapeutics-induced mucositis (CIM) period (Table 1) and the 225 min single-pass perfusion period (75 min resting and 150 min experiment). The intestinal mannitol permeability was monitored during the whole 150 min experimental period. DOX-doxorubicin, 5-FU—5-Fluorouracil, IRI—irinotecan, SDS—sodium dodecyl sulfate, EtOH—Ethanol.

Following the 60 min resting period, three different SPIP experiments were performed while continuously monitoring the intestinal mannitol permeability (Figure 7). In one SPIP experiment, containing 6 of the 18 control rats, the control buffer solution was perfused during 120 min. The other two SPIP experiments were divided into three periods, in which

both of them contained six rats from each of the four treatment arms (control, DOX, IRI, and 5-FU; see Table 1). Initially, (i) the jejunal segment was perfused with the control solution for 60 min to establish baseline permeability in each rat. This was directly followed by (ii) a 15 min perfusion with 5 mg/mL SDS or 15% ethanol to evaluate their effect on mucosal permeability and histology. Finally, (iii) the control buffer solution was again perfused for 60 min, during which time the recovery of the mucosa was evaluated. This experimental setup allowed us to evaluate the effect of chemotherapy on basal mucosal mannitol permeability (0–75 min), as well as the ability of the jejunal mucosa to respond to luminal irritants 72 h after chemotherapy (75–150 min).

All experimental periods started with a rapid filling (<20 s) of the entire jejunal segment with the perfusate (about 1.5 mL for a 10 cm segment). Thereafter, the single-pass perfusion rate was always 0.2 mL/min (peristaltic pump, Gilson Minipuls 3, Le Bel, France). The jejunal segment and perfusates were kept at 37 °C, and all outgoing perfusate was collected and weighed at 15 min intervals. The length and wet tissue weight of each jejunal segment was determined after the experiment. Blood samples (<0.3 mL) were drawn from the femoral artery before the start (t = 0 min) and then again at the end (t = 150 min) of the perfusion experiment. The blood samples were centrifuged (5000× g, 3 min at 4 °C) within 10 min, and the plasma was analyzed for ^{3}H activity.

4.5. Determination of Blood-to-Lumen Jejunal ^{3}H-Mannitol Clearance

In the SPIP experiments, 2 mL scintillation fluid (Pico-Fluor Plus, Perkin Elmer Life Sciences, Boston, MA, USA) was added to the luminal perfusates (1 mL), and the 0 and 150 min plasma samples (0.05 mL plasma with 0.95 mL water). These samples were then analyzed for ^{3}H-mannitol in a scintillator (Tri-Carb 2910 TR, Perkin Elmer Life Sciences, Boston, MA, USA). Linear regression analysis of the plasma samples was made to obtain a corresponding plasma value for each perfusate sample. The blood-to-lumen mannitol clearance ($CL_{mannitol}$) was calculated using Equation (1) [16].

$$CL_{mannitol} = \frac{C_{perfusate} \times Q_{in}}{C_{plasma} \times \text{tissue weight}} \times 100 \tag{1}$$

$C_{perfusate}$ and C_{plasma} is the activity in the perfusate and plasma per mL, and Q_{in} is the flow rate in mL per min. In each group, $CL_{mannitol}$ values over time (0 to 150 min) are calculated from the perfusion experiments: 0–75 min are the baseline mannitol permeability, and 75–150 min are the effects of the luminal irritants on mannitol permeability relative to the baseline period.

4.6. Histology

Two jejunal samples from each rat were collected for histology. One sample, adjacent to the perfused segment, was excised before the experiment. The other was excised from within the perfused segment, immediately after the end of the perfusion. These samples allowed us to evaluate the histological effects of chemotherapeutics, with and without luminal irritants (control, SDS and ethanol). The tissue samples were rinsed with saline and fixed in 10% formaldehyde for 24 h then transferred to 70% ethanol. They were then embedded in paraffin and microtome-sliced (Microm Cool-Cut HM 355 S, Thermo Fisher Scientific, Waltham, MA, USA) at 8 µm and dried overnight. Sections were de-paraffinized and rehydrated prior to staining. Hematoxylin-eosin staining was carried out according to standard practice [46].

The histological samples were analyzed for villi length and crypt depth, which were taken as measures of mucositis. Ten villi and crypts were measured (Figure 8) for each rat, and the mean was chosen as representative for that animal. Images were taken using an inverted confocal microscope (Eclipse TE2000-U, Nikon, Tokyo, Japan). The measurements were performed using the corresponding plugin in the ImageJ software version 1.50e (NIH, Bethesda, Maryland, USA).

Figure 8. Method by which the villus length (finger-like protrusions) and crypt depth (area between villus bottom and muscle layer) were measured in each rat. The arrows show the length of each villus and crypt. The average of ten measurements was used for each animal.

4.7. Statistics

All data are expressed as mean $\pm$ SD or SEM. The villi length, crypt depth, villi:crypt ratio, basal $CL_{mannitol}$, and $CL_{mannitol}$ were analyzed directly after the end of the perfusion with luminal ethanol and SDS (t = 90 min). Rats dosed with DOX, IRI, and 5-FU were compared against the controls using a one-way, unpaired ANOVA, with a post hoc Dunnett's comparison test. A *p*-value < 0.05 was regarded as significant in all analyses. Statistic tests and graphs were made in GraphPad Prism 9.1.2 (La Jolla, CA, USA).

Author Contributions: Conceptualization, M.-J.C.-C., D.D., F.K., K.P., T.O., M.S. and H.L.; methodology, M.-J.C.-C. and T.O.; software, M.-J.C.-C., D.D., F.K., K.P., T.O., M.S. and H.L.; validation, M.-J.C.-C., D.D., F.K., K.P., T.O., M.S. and H.L.; formal analysis, M.-J.C.-C., D.D., F.K., K.P., T.O., M.S. and H.L.; investigation, M.-J.C.-C., D.D., F.K., K.P., T.O., M.S. and H.L.; resources, H.L.; data curation, M.-J.C.-C., D.D., F.K., K.P., T.O., M.S. and H.L.; writing—original draft preparation, M.S. and D.D.; writing—review and editing, M.-J.C.-C., D.D., F.K., K.P., T.O., M.S. and H.L.; visualization, M.-J.C.-C., D.D., F.K., K.P., T.O., M.S. and H.L.; supervision, D.D. and H.L.; project administration, M.-J.C.-C., D.D., M.S. and H.L.; funding acquisition, M.S. and H.L. All authors have read and agreed to the published version of the manuscript.

Institutional Review Board Statement: This rat study was approved by the local ethics committee for animal research (5.8.18-17754/2019) in Uppsala, Sweden.

Informed Consent Statement: Not applicable.

Data Availability Statement: The data presented in this study are available on request from the corresponding author.

Conflicts of Interest: The authors declare no conflict of interest.

References

1. Bray, F.; Laversanne, M.; Weiderpass, E.; Soerjomataram, I. The ever-increasing importance of cancer as a leading cause of premature death worldwide. *Cancer* **2021**, *127*, 3029–3030. [CrossRef]
2. Darwich, A.S.; Aslam, U.; Ashcroft, D.M.; Rostami-Hodjegan, A. Meta-analysis of the turnover of intestinal epithelia in preclinical animal species and humans. *Drug Metab. Dispos.* **2014**, *42*, 2016–2022. [CrossRef]
3. Dahlgren, D.; Sjöblom, M.; Hellström, P.M.; Lennernäs, H. Chemotherapeutics-induced intestinal mucositis: Pathophysiology and potential treatment strategies. *Front. Pharmacol.* **2021**, *12*, 1020. [CrossRef]
4. Keefe, D.M.; Elting, L.S.; Nguyen, H.T.; Grunberg, S.M.; Aprile, G.; Bonaventura, A.; Selva-Nayagam, S.; Barsevick, A.; Koczwara, B.; Sonis, S.T. Risk and outcomes of chemotherapy-induced diarrhea (CID) among patients with colorectal cancer receiving multi-cycle chemotherapy. *Cancer Chemother. Pharmacol.* **2014**, *74*, 675–680. [CrossRef]
5. Helander, H.F.; Fändriks, L. Surface area of the digestive tract-revisited. *Scand. J. Gastroenterol.* **2014**, *49*, 681–689. [CrossRef]

6. Avritscher, E.B.; Cooksley, C.D.; Elting, L.S. Scope and epidemiology of cancer therapy-induced oral and gastrointestinal mucositis. *Proc. Semin. Oncol. Nurs.* **2004**, *20*, 3–10. [CrossRef]

7. Menzies, I.S. Absorption of intact oligosaccharide in health and disease. *Biochem. Soc. Trans.* **1974**, *2*, 1042–1047. [CrossRef]

8. Vilela, E.; Torres, H.; Ferrari, M.; Lima, A.; Cunha, A. Gut permeability to lactulose and mannitol differs in treated Crohn's disease and celiac disease patients and healthy subjects. *Braz. J. Med. Biol. Res.* **2008**, *41*, 1105–1109. [CrossRef]

9. Bjarnason, I.; Macpherson, A.; Hollander, D. Intestinal permeability: An overview. *Gastroenterology* **1995**, *108*, 1566–1581. [CrossRef]

10. Tooley, K.L.; Howarth, G.S.; Butler, R.N. Mucositis and non-invasive markers of small intestinal function. *Cancer Biol. Ther.* **2009**, *8*, 753–758. [CrossRef]

11. Camilleri, M. Leaky gut: Mechanisms, measurement and clinical implications in humans. *Gut* **2019**, *68*, 1516–1526. [CrossRef] [PubMed]

12. Berg, R.D. Bacterial translocation from the gastrointestinal tract. *Mech. Pathog. Enteric Dis. 2* **1999**, *473*, 11–30.

13. Sommansson, A.; Saudi, W.S.W.; Nylander, O.; Sjöblom, M. Melatonin inhibits alcohol-induced increases in duodenal mucosal permeability in rats in vivo. *Am. J. Physiol.-Gastrointest. Liver Physiol.* **2013**, *305*, G95–G105. [CrossRef] [PubMed]

14. Dahlgren, D.; Roos, C.; Lundqvist, A.; Tannergren, C.; Sjöblom, M.; Sjögren, E.; Lennernäs, H. Time-dependent effects on small intestinal transport by absorption-modifying excipients. *Eur. J. Pharm. Biopharm.* **2018**, *132*, 19–28. [CrossRef]

15. Rubbens, J.; Brouwers, J.; Wolfs, K.; Adams, E.; Tack, J.; Augustijns, P. Ethanol concentrations in the human gastrointestinal tract after intake of alcoholic beverages. *Eur. J. Pharm. Sci.* **2016**, *86*, 91–95. [CrossRef]

16. Dahlgren, D.; Roos, C.; Lundqvist, A.; Langguth, P.; Tannergren, C.; Sjöblom, M.; Sjögren, E.; Lennernas, H. Preclinical effect of absorption modifying excipients on rat intestinal transport of five model compounds and the intestinal barrier marker 51Cr-EDTA. *Mol. Pharm.* **2017**, *14*, 4243–4251. [CrossRef]

17. Blikslager, A.T.; Moeser, A.J.; Gookin, J.L.; Jones, S.L.; Odle, J. Restoration of barrier function in injured intestinal mucosa. *Physiol. Rev.* **2007**, *87*, 545–564. [CrossRef]

18. Peters, K.; Dahlgren, D.; Lennernäs, H.; Sjöblom, M. Melatonin-activated receptor signaling pathways mediate protective effects on surfactant-induced increase in jejunal mucosal permeability in rats. *Int. J. Mol. Sci.* **2021**, *22*, 10762. [CrossRef]

19. Thomsen, M.; Vitetta, L. Adjunctive treatments for the prevention of chemotherapy-and radiotherapy-induced mucositis. *Integr. Cancer Ther.* **2018**, *17*, 1027–1047. [CrossRef]

20. Billeschou, A.; Hunt, J.; Kissow, H. Important endpoints and proliferative markers to assess small intestinal injury and adaptation using a mouse model of chemotherapy-induced mucositis. *JoVE J. Vis. Exp.* **2019**, e59236. [CrossRef]

21. Wardill, H.R.; Bowen, J.M.; Al-Dasooqi, N.; Sultani, M.; Bateman, E.; Stansborough, R.; Shirren, J.; Gibson, R.J. Irinotecan disrupts tight junction proteins within the gut: Implications for chemotherapy-induced gut toxicity. *Cancer Biol. Ther.* **2014**, *15*, 236–244. [CrossRef]

22. Menzies, I.; Pounder, R.; Heyer, S.; Laker, M.; Bull, J.; Wheeler, P.; Creamer, B. Abnormal intestinal permeability to sugars in villous atrophy. *Lancet* **1979**, *314*, 1107–1109. [CrossRef]

23. Fihn, B.M.; Sjöqvist, A.; Jodal, M. Permeability of the rat small intestinal epithelium along the villus-crypt axis: Effects of glucose transport. *Gastroenterology* **2000**, *119*, 1029–1036. [CrossRef] [PubMed]

24. Dahlgren, D.; Cano-Cebrián, M.-J.; Olander, T.; Hedeland, M.; Sjöblom, M.; Lennernas, H. Regional intestinal drug permeability and effects of permeation enhancers in rat. *Pharmaceutics* **2020**, *12*, 242. [CrossRef]

25. Dahlgren, D.; Lennernäs, H. Intestinal permeability and drug absorption: Predictive experimental, computational and in vivo approaches. *Pharmaceutics* **2019**, *11*, 411. [CrossRef] [PubMed]

26. Dahlgren, D.; Cano-Cebrián, M.-J.; Hellström, P.M.; Wanders, A.; Sjöblom, M.; Lennernäs, H. Prevention of rat intestinal injury with a drug combination of melatonin and misoprostol. *Int. J. Mol. Sci.* **2020**, *21*, 6771. [CrossRef] [PubMed]

27. Sedin, J.; Dahlgren, D.; Sjöblom, M.; Nylander, O. The Impact of alpha-adrenoceptors in the regulation of the hypotonicity-induced increase in duodenal mucosal permeability in vivo. *Pharmaceutics* **2021**, *13*, 2096. [CrossRef]

28. Sangild, P.T.; Shen, R.L.; Pontoppidan, P.; Rathe, M. Animal models of chemotherapy-induced mucositis: Translational relevance and challenges. *Am. J. Physiol.-Gastrointest. Liver Physiol.* **2018**, *314*, G231–G246. [CrossRef] [PubMed]

29. Kaczmarek, A.; Brinkman, B.M.; Heyndrickx, L.; Vandenabeele, P.; Krysko, D.V. Severity of doxorubicin-induced small intestinal mucositis is regulated by the TLR-2 and TLR-9 pathways. *J. Pathol.* **2012**, *226*, 598–608. [CrossRef]

30. Capaldo, C.T.; Nusrat, A. Cytokine regulation of tight junctions. *Biochim. Biophys. Acta (BBA)-Biomembr.* **2009**, *1788*, 864–871. [CrossRef]

31. Melo, M.L.P.; Brito, G.A.; Soares, R.C.; Carvalho, S.B.; Silva, J.V.; Soares, P.M.; Vale, M.L.; Souza, M.H.; Cunha, F.Q.; Ribeiro, R.A. Role of cytokines (TNF-α, IL-1β and KC) in the pathogenesis of CPT-11-induced intestinal mucositis in mice: Effect of pentoxifylline and thalidomide. *Cancer Chemother. Pharmacol.* **2008**, *61*, 775–784. [CrossRef]

32. Hamouda, N.; Sano, T.; Oikawa, Y.; Ozaki, T.; Shimakawa, M.; Matsumoto, K.; Amagase, K.; Higuchi, K.; Kato, S. Apoptosis, dysbiosis and expression of inflammatory cytokines are sequential events in the development of 5-fluorouracil-induced intestinal mucositis in mice. *Basic Clin. Pharmacol. Toxicol.* **2017**, *121*, 159–168. [CrossRef]

33. Beukema, M.; Jermendi, É.; Koster, T.; Kitaguchi, K.; de Haan, B.J.; van den Berg, M.A.; Faas, M.M.; Schols, H.A.; de Vos, P. Attenuation of doxorubicin-induced small intestinal mucositis by pectins is dependent on pectin's methyl-ester number and distribution. *Mol. Nutr. Food Res.* **2021**, *65*, 2100222. [CrossRef]

34. Ferreira, T.M.; Leonel, A.J.; Melo, M.A.; Santos, R.R.; Cara, D.C.; Cardoso, V.N.; Correia, M.I.; Alvarez-Leite, J.I. Oral supplementation of butyrate reduces mucositis and intestinal permeability associated with 5-fluorouracil administration. *Lipids* **2012**, *47*, 669–678. [CrossRef] [PubMed]

35. Melichar, B.; Zezulová, M. The significance of altered gastrointestinal permeability in cancer patients. *Curr. Opin. Supportive Palliat. Care* **2011**, *5*, 47–54. [CrossRef]

36. Stein, A.; Voigt, W.; Jordan, K. Chemotherapy-induced diarrhea: Pathophysiology, frequency and guideline-based management. *Ther. Adv. Med. Oncol.* **2010**, *2*, 51–63. [CrossRef] [PubMed]

37. Odenwald, M.A.; Turner, J.R. The intestinal epithelial barrier: A therapeutic target? *Nat. Rev. Gastroenterol. Hepatol.* **2017**, *14*, 9. [CrossRef] [PubMed]

38. Muehler, A.; Slizgi, J.R.; Kohlhof, H.; Groeppel, M.; Peelen, E.; Vitt, D. Clinical relevance of intestinal barrier dysfunction in common gastrointestinal diseases. *World J. Gastrointest. Pathophysiol.* **2020**, *11*, 114. [CrossRef]

39. Sommansson, A.; Saudi, W.S.W.; Nylander, O.; Sjöblom, M. Effects of melatonin in ethanol-induced increases in duodenal mucosal permeability, motility and bicarbonate secretion in rats. *Proc. Acta Physiol.* **2015**, *214*, 2–3.

40. Pihl, L.; Wilander, E.; Nylander, O. Comparative study of the effect of luminal hypotonicity on mucosal permeability in rat upper gastrointestinal tract. *Acta Physiol.* **2008**, *193*, 67–78. [CrossRef]

41. Dahlgren, D.; Sjöblom, M.; Hedeland, M.; Lennernäs, H. The in vivo effect of transcellular permeation enhancers on the intestinal permeability of two peptide drugs enalaprilat and hexarelin. *Pharmaceutics* **2020**, *12*, 99. [CrossRef] [PubMed]

42. Gibson, R.J.; Bowen, J.M.; Inglis, M.R.; Cummins, A.G.; Keefe, D.M. Irinotecan causes severe small intestinal damage, as well as colonic damage, in the rat with implanted breast cancer. *J. Gastroenterol. Hepatol.* **2003**, *18*, 1095–1100. [CrossRef] [PubMed]

43. Blandizzi, C.; De Paolis, B.; Colucci, R.; Lazzeri, G.; Baschiera, F.; Del Tacca, M. Characterization of a novel mechanism accounting for the adverse cholinergic effects of the anticancer drug irinotecan. *Br. J. Pharmacol.* **2001**, *132*, 73–84. [CrossRef] [PubMed]

44. Gibson, R.J.; Bowen, J.M.; Alvarez, E.; Finnie, J.; Keefe, D.M. Establishment of a single-dose irinotecan model of gastrointestinal mucositis. *Chemotherapy* **2007**, *53*, 360–369. [CrossRef]

45. Dahlgren, D.; Roos, C.; Peters, K.; Lundqvist, A.; Tannergren, C.; Sjögren, E.; Sjöblom, M.; Lennernäs, H. Evaluation of drug permeability calculation based on luminal disappearance and plasma appearance in the rat single-pass intestinal perfusion model. *Eur. J. Pharm. Biopharm.* **2019**, *142*, 31–37. [CrossRef]

46. Cardiff, R.D.; Miller, C.H.; Munn, R.J. Manual hematoxylin and eosin staining of mouse tissue sections. *Cold Spring Harb. Protoc.* **2014**, *6*, 655–658. [CrossRef]